

RD-R194 503

TE/TM (TRANSVERSE MAGNETIC/TRANSVERSE ELECTRIC) HEIGHT  
PROFILE MEASUREMENTS (U) ROME AIR DEVELOPMENT CENTER  
GRIFFISS AFB NY J P TURTLE ET AL. OCT 87

1/1

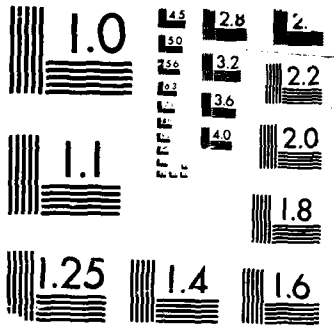
UNCLASSIFIED

RADC-TR-87-207

F/G 20/14

NL





MICROCOPY RESOLUTION TEST CHART  
ORFAU C-1 STANDARDS 1963-A

AD-A194 503

RADC-TR-87-207  
In-House Report  
October 1987

DTIC FILE COPY



(4)

# TE/TM HEIGHT PROFILE MEASUREMENTS OF TRANSPOLAR VLF SIGNALS

John P. Turtle, John L. Heckscher and Paul A. Kossey

DTIC  
ELECTED  
JUN 27 1988  
S D  
GND

APPROVED FOR PUBLIC RELEASE; DISTRIBUTION UNLIMITED.

This effort was sponsored by the Defense Nuclear Agency.

ROME AIR DEVELOPMENT CENTER  
Air Force Systems Command  
Griffiss Air Force Base, NY 13441-5700

88 6 27 02

Unclassified

SECURITY CLASSIFICATION OF THIS PAGE

APR 6 1988  
REPORT DOCUMENTATION PAGE

1a. REPORT SECURITY CLASSIFICATION <b>Unclassified</b>		1b. RESTRICTIVE MARKINGS										
2a. SECURITY CLASSIFICATION AUTHORITY		3. DISTRIBUTION / AVAILABILITY OF REPORT <b>Approved for Public Release; Distribution unlimited</b>										
2b. DECLASSIFICATION / DOWNGRADING SCHEDULE		5. MONITORING ORGANIZATION REPORT NUMBER(S)										
4. PERFORMING ORGANIZATION REPORT NUMBER(S)  <b>RADC-TR-87-207</b>		7a. NAME OF MONITORING ORGANIZATION  <b>Rome Air Development Center (EECP)</b>										
6a. NAME OF PERFORMING ORGANIZATION  <b>Rome Air Development Center</b>	6b. OFFICE SYMBOL (If applicable)  <b>EECP</b>	7b. ADDRESS (City, State, and ZIP Code)  <b>Hanscom AFB Massachusetts 01731-5000</b>										
8a. NAME OF FUNDING/SPONSORING ORGANIZATION  <b>Defense Nuclear Agency</b>	8b. OFFICE SYMBOL (If applicable)  <b>RAAE</b>	9. PROCUREMENT INSTRUMENT IDENTIFICATION NUMBER										
8c. ADDRESS (City, State, and ZIP Code)  <b>Washington, DC 10305</b>		10. SOURCE OF FUNDING NUMBERS  <table border="1"><tr><td>PROGRAM ELEMENT NO.  <b>62715H</b></td><td>PROJECT NO.  <b>R248</b></td><td>TASK NO.  <b>00</b></td><td>WORK UNIT ACCESSION NO.  <b>01</b></td></tr></table>		PROGRAM ELEMENT NO.  <b>62715H</b>	PROJECT NO.  <b>R248</b>	TASK NO.  <b>00</b>	WORK UNIT ACCESSION NO.  <b>01</b>					
PROGRAM ELEMENT NO.  <b>62715H</b>	PROJECT NO.  <b>R248</b>	TASK NO.  <b>00</b>	WORK UNIT ACCESSION NO.  <b>01</b>									
11. TITLE (Include Security Classification)  <b>TE/TM Height Profile Measurements of Transpolar VLF Signals</b>												
12. PERSONAL AUTHOR(S) <b>Turtle, John P., Heckscher, John L., * Kossey, Paul A. *</b>												
13a. TYPE OF REPORT <b>In-House</b>	13b. TIME COVERED FROM _____ TO _____	14. DATE OF REPORT (Year, Month, Day) <b>1987 October</b>	15. PAGE COUNT <b>32</b>									
16. SUPPLEMENTARY NOTATION  <b>*AFGL/LID, Hanscom AFB, MA 01731-5000. This work was sponsored by the (cont.)</b>												
17. COSATI CODES <table border="1"><tr><th>FIELD</th><th>GROUP</th><th>SUB-GROUP</th></tr><tr><td>17</td><td>02</td><td></td></tr><tr><td>21</td><td>14</td><td></td></tr></table>	FIELD	GROUP	SUB-GROUP	17	02		21	14		18. SUBJECT TERMS (Continue on reverse if necessary and identify by block number)  <b>Very low frequency Waveguide propagation Communications</b>		
FIELD	GROUP	SUB-GROUP										
17	02											
21	14											
19. ABSTRACT (Continue on reverse if necessary and identify by block number)  <b>Transverse magnetic (TM) and transverse electric (TE) height-gain profiles of eight ground-based transmitters and one airborne transmitter were measured simultaneously by a rocket-borne wideband receiver flown at Thule AB, Greenland, under nighttime conditions. The profile shapes are shown to depend both on ground parameters and on solar illumination conditions over the propagation paths. Significant TM-to-TE conversion was observed for ground-based transmitters located in the night hemisphere, while none was measured for sources in daylight. No TE-to-TM conversion was measured for the airborne transmitter.</b>												
20. DISTRIBUTION / AVAILABILITY OF ABSTRACT <input checked="" type="checkbox"/> UNCLASSIFIED/UNLIMITED <input type="checkbox"/> SAME AS RPT <input type="checkbox"/> DTIC USERS		21. ABSTRACT SECURITY CLASSIFICATION <b>Unclassified</b>										
22a. NAME OF RESPONSIBLE INDIVIDUAL <b>John P. Turtle</b>		22b. TELEPHONE (Include Area Code) <b>(617) 377-2988</b>	22c. OFFICE SYMBOL <b>RADC/EECP</b>									

**Unclassified**

**Block 16 (cont.).**

**Defense Nuclear Agency under Project/Task I25AMXIO, Work Unit 00071.**

## Preface

Funding for this effort was provided, in part, by the Atmospheric Effects Branch, Defense Nuclear Agency (DNA/RAAE) and by the Air Force Support to MEECN System Project Office, Electronic Systems Division (ESD/SCS-2).

The authors thank D. Mark Haines for design assistance with the rocket instrumentation, Edward C. Field, Jr., for guidance in interpretation of the data, Martin Allerding, Major, USA, for continued advocacy and fiscal support, and the TACAMO flight crews from Fleet Air Reconnaissance Squadron Four for airborne transmissions.

Appreciation also is extended to the Danish Commission for Scientific Research in Greenland for permission to conduct the launches; to Aage Paulsen and the ARCAS launch crew at Thule AB; to the operational staff of the Thule Tracking Site of the AF Satellite Control Facility for providing tracking and telemetry support as well as working space; and to Jorgen Taagholt, the Danish Scientific Liaison Officer for Greenland and V. Neble Jensen of the Geophysics Division of the Danish Meteorological Institute for their continued cooperation.



Accession For	
NTIS CRAXI <input checked="" type="checkbox"/>	
DTIC TAB <input type="checkbox"/>	
Data Enclosed <input type="checkbox"/>	
Index Attached <input type="checkbox"/>	
By _____	
Date _____	
Availability Codes	
A-1	

## **Contents**

1. INTRODUCTION	1
2. INSTRUMENTATION	3
3. TRAJECTORY AND ATTITUDE ANALYSIS	5
4. DATA REDUCTION	10
5. SIGNAL SOURCES, LOCATIONS, AND PROPAGATION PATHS	11
6. HEIGHT PROFILES	13
7. DATA ANALYSIS AND DISCUSSION	14
8. CONCLUSIONS	20
REFERENCES	25

## **Illustrations**

1. Rocket Payload Showing Major Components	4
2. Rocket Instrumentation for Measuring TM and TE Height-Gain Profiles	5
3. Ground-Based Instrumentation for Recording TM and TE Height-Gain Profiles	6
4. Coordinate System for the Rocket Trajectory	7

## **Illustrations**

5. Data Reduction Flow Chart for Mode Profile Analysis	10
6. Composite Spectrum of Received TM Signals	11
7. Propagation Paths to Thule	12
8. Height-Gain Profiles for 16.4 kHz (JXZ)	14
9. Height-Gain Profiles for 17.1 kHz (UMS)	15
10. Height-Gain Profiles for 17.8 kHz (NAA)	16
11. Height-Gain Profiles for 19.05 kHz (GQD)	17
12. Height-Gain Profiles for 19.6 kHz (GBZ)	18
13. Height-Gain Profiles for 21.4 kHz (NSS)	19
14. Height-Gain Profiles for 23.4 kHz (NPM)	20
15. Height-Gain Profiles for 24.8 kHz (NLK)	21
16. Height-Gain Profiles for 26.1 kHz (TACAMO)	22
17. Calculated Height-Gain Profiles for GBZ to Thule	23

## **Tables**

1. Transmitter Listing by Frequency	13
2. Propagation Conditions	23

## **TE/TM Height Profile Measurements of Transpolar VLF Signals**

### **1. INTRODUCTION**

Because low and very low frequency (LF/VLF) radio signals propagate with relatively low attenuation within the Earth-ionosphere waveguide, they are used extensively for very long range, survivable communications. Conventional LF/VLF systems employ large, vertical transmitting antennas that radiate transverse magnetic (TM) waves. Recently, it has become practical to radiate LF/VLF energy from the aircraft, the TWAs are unspooled to lengths approaching half-wave resonance, making them very efficient radiators. Due to air drag, the TWAs are nearly horizontal, so they couple to transverse electric (TE) modes as well as to the TM modes. TE signals have fields that tend to be very weak near the ground and strong at aircraft altitudes, while TM signals tend to be strongest near the ground. Thus, there is increasing interest in exploiting polarization diversity (the combination of TE and TM modes) to enhance air-to-air capabilities of the Minimum Essential Emergency Communications Network (MEECN).

Although well-understood theoretically, TE signals have not been measured nearly as extensively as those of the more commonly used TM modes. In the mid-1970s, the Rome Air Development Center (RADC) conducted a series of balloon

---

(Received for publication 14 October 1987)

probe experiments in which TE and TM field strength profiles of a number of ground-based and airborne LF/VLF transmitters were measured to altitudes of about 20 km.<sup>1</sup> RADC also equipped a U-2 aircraft to measure how TE and TM signals varied with range from airborne transmitters.<sup>2</sup> In 1979, the first of a series of Super ARCAS rocket probes carrying LF/VLF sensors was launched from the NASA Wallops Flight Center, Wallops Island, Virginia, to sample the TE and TM noise environment.<sup>3</sup> Subsequent launches observed height profiles of TE/TM signals from airborne terminals at long distances over sea water.<sup>4</sup> A comprehensive review of the results from these and other experiments was presented at a meeting of the Electromagnetic Wave Propagation Panel of AGARD in Brussels, Belgium, in 1981.<sup>5</sup>

With the continuing development and upgrade of low frequency components of MEECN, including the modernization of TWA transmitters on the Airborne Command Posts (ABNCP) as well as the incorporation of Miniature Receive Terminals (MRT) on-board strategic bombers, an adequate database pertaining to LF/VLF signal propagation and noise in the polar regions at aircraft altitudes becomes critically important. Of special concern are the characteristics of TE and TM modes propagating over poorly conducting arctic regions, under both normal and disturbed ionospheric conditions. Under sponsorship of the Defense Nuclear Agency Agency (DNA) and the Electronic Systems Division (ESD), RADC conducted rocket experiments in 1983, using standard ARCAS rockets launched from Thule AB, Greenland, to measure height profiles of TE and TM signals and noise within the polar cap to altitudes of about 60 km.

This report presents the results obtained from a rocket flight launched at 0600 UT on 21 September 1983 under quiet ionospheric conditions. The payload

---

1. Lewis, E.A., and Harrison, R.P. (1975) Experimental Evidence of a Strong TE-Polarized Wave From an Airborne LF Transmitter, AFCRL-TR-75-0555, AD A019689.
2. Hirst, G.C. (1975) (U) U-2 investigations of a new mode for LF air-to-air communications, in Proc. AFSC 1975 Science and Engineering Symposium, AFSC-TR-75-06 (Vol. 1), AD A021660.
3. Harrison, R.P., Lewis, E.A., Donohoe, J.B., and Rasmussen, J.E. (1981) TM/TE Polarization Ratios in a Sample of 30 kHz Sferics Received at Altitudes From 0 to 70 km, RADC-TR-81-235, AD A108182.
4. Field, E.C., Jr., Warber, C.R., Kossey, P.A., Lewis, E.A., and Harrison, R.P. (1986) Comparison of calculated and measured height profiles of transverse electric VLF signals across the daytime Earth-ionosphere waveguide, Radio Sci. 21(No. 1):141-149.
5. Kossey, P.A., Lewis, E.A., and Field, E.C. (1982) Relative characteristics of TE/TM waves excited by airborne VLF/LF transmitters, in Medium, Long and Very Long Wave Propagation (at frequencies less than 3000 kHz), AGARD-CP-305, Dr. J.S. Belrose, Advisory Group for Aerospace Research and Development, North Atlantic Treaty Organization, ed., AD A113969.

and ground-based instrumentation are described, the trajectory and attitude orientation compensations applied to the raw data are derived, and TM and TE height profiles for a number of ground and airborne LF/VLF transmitters are presented and discussed.

## 2. INSTRUMENTATION

The rocket payload (Figure 1) was designed with two separate receiving channels, to measure orthogonal magnetic field components of incident waves. Space considerations required the antenna mounted transverse to the rocket axis (the "TM channel") to be constructed of two separate 10.2 cm-long ferrite cores, each with 350 turns, connected in series, while the longitudinal antenna (the "TE channel") was made of one continuous 20.3 cm length of ferrite with 650 turns. A fiber-glass nosecone covered the antennas during flight. The difference in physical length, and, therefore, the sensitivity, between the two antennas was calibrated by placing the payload (without the ARCAS body) in a radio frequency magnetic field of known strength.

Each antenna was connected to a high-gain, broadband (15 to 50 kHz, 3 dB bandwidth) amplifier whose output frequency-modulated a separate sub-carrier oscillator (VCO in Figure 2). The two sub-carrier signals then were mixed to form a composite that, in turn, frequency-modulated a 100 mW S-Band (2252.5 MHz) telemetry transmitter with its associated slot antenna. A 1 MHz oscillator signal also was mixed into the composite signal, to provide a method for estimating slant range to the rocket payload during its flight.

The telemetry receiving system and associated ground-based instrumentation are shown in Figure 3. At Thule AB, the telemetry antenna, S-band receiver, FM discriminator, and tape recorder were supplied by Det 3 of the Air Force Satellite Control Facility (AFSCF). The video output of the telemetry receiver corresponded to the composite signal (sub-carriers plus 1 MHz sine wave) present at the input of the rocket transmitter. Replicas of the original TE and TM signals present at the output of the broadband amplifier, as well as the 1 MHz oscillator signal in the rocket, were obtained by filtering and processing through FM discriminators; these replicas were recorded on separate analog tape tracks to preserve the bandwidth of the two rocket data channels and allow post-flight processing in different ways, depending on the study requirements.

To estimate the slant range and thus derive altitude, the 1 MHz replica was input to the "A" channel of a two-channel oscilloscope, while another 1 MHz signal derived from a local source was applied to the "B" channel. In the "A + B" mode, the oscilloscope sums the two signals; the two oscillators are brought into syn-

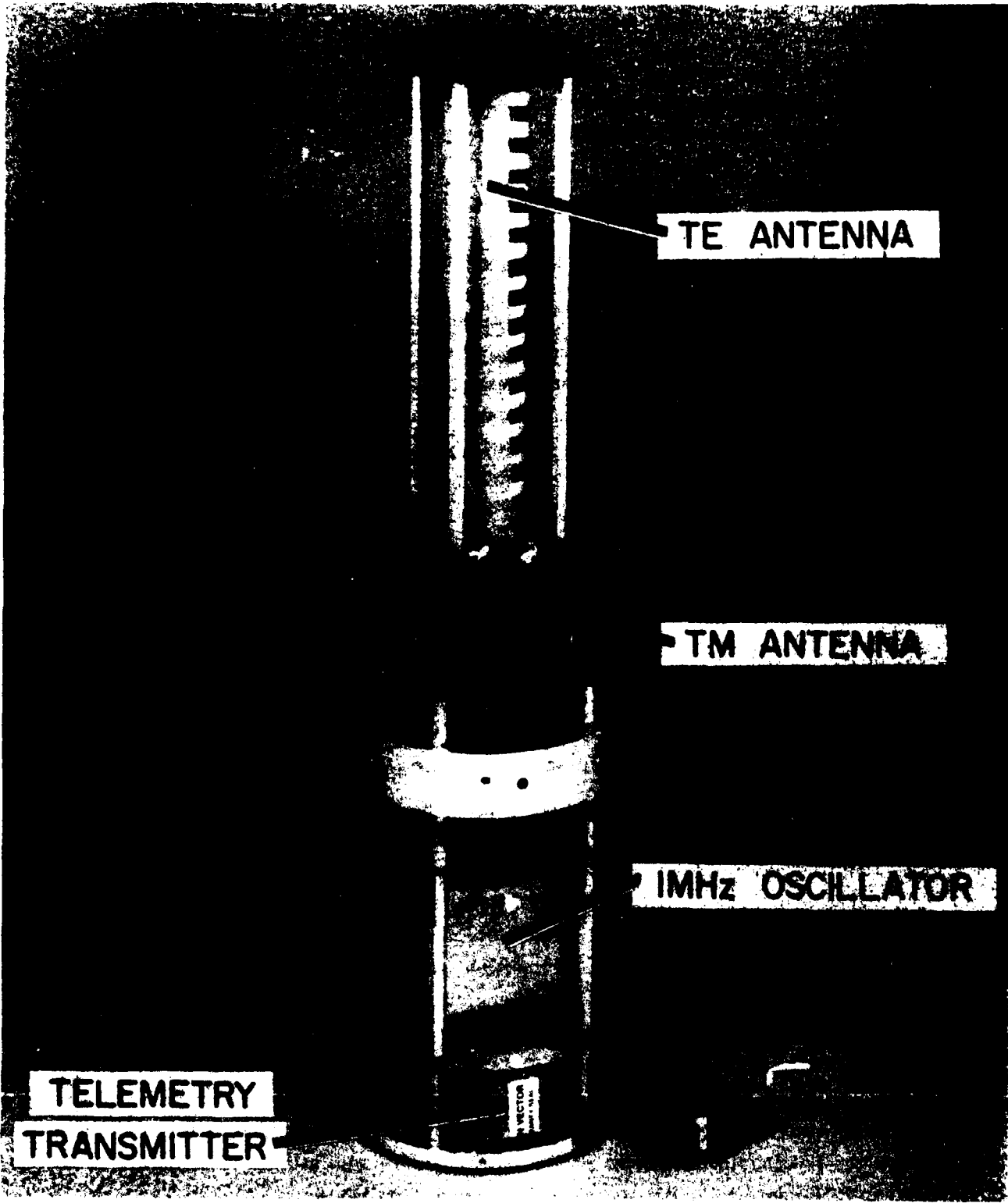


Figure 1. Rocket Payload Showing Major Components

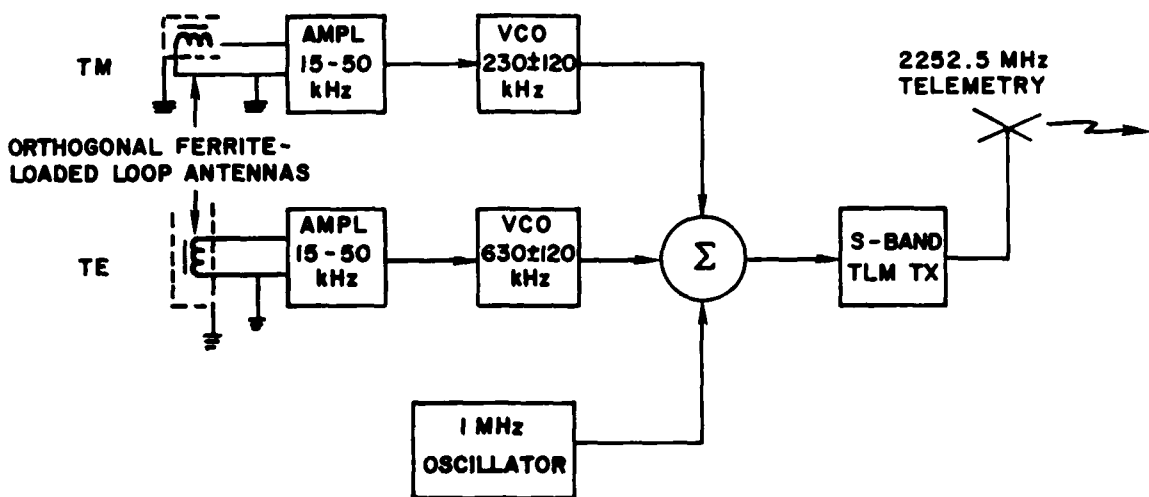


Figure 2. Rocket Instrumentation for Measuring TM and TE Height-Gain Profiles. The 1 MHz oscillator provides a signal for estimating slant range from the telemetry/tracking antenna

chronism by adjusting the phase of the ground-based source to give a steady presentation while the rocket is still on the ground in the launcher. During flight, the phase of the 1 MHz replica lags that of the local oscillator due to the increase in distance; by counting the cycles of phase shift, the change in distance could be determined.

A tunable narrowband receiver with a vertical loop antenna was also operated in conjunction with the rocket flight. This was used to measure, at ground level, the signals from several of the transmitters monitored by the rocket-borne receivers.

### 3. TRAJECTORY AND ATTITUDE ANALYSIS

#### The ARCAS flight trajectory

$$T(x, y, z) = [x(t), y(t), z(t)] \quad (1)$$

can be determined from measurements of azimuth,  $\varphi$ , and elevation,  $\theta$ , supplied by AFSCF in printout form, combined with estimates of slant range,  $R$ , obtained from a count of cycle slips between the 1 MHz oscillator on the rocket and a local 1 MHz oscillator. For 1 MHz, a change of one cycle corresponds to a change in slant range of 0.3 km. The Cartesian coordinates can be found using

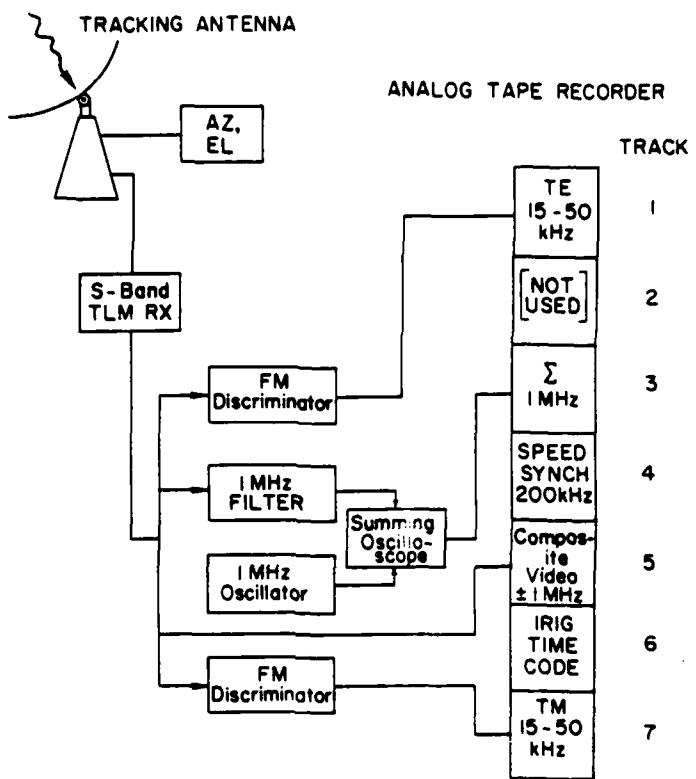


Figure 3. Ground-Based Instrumentation for Recording TM and TE Height-Gain Profiles. The rocket trajectory is computed using azimuth and elevation from the tracking antenna in combination with range estimated from the rocket 1 MHz phase lag

$$\begin{aligned}
 x(t) &= R \cos \theta \cos \varphi \\
 y(t) &= R \cos \theta \sin \varphi \\
 z(t) &= R \sin \theta
 \end{aligned} \tag{2}$$

where the origin of coordinates is the tracking station (see Figure 4).

A sounding rocket trajectory approximates a parabola in the plane determined by the burn-out coordinates, the apogee, and the impact point. In the x-z plane, a parabolic trajectory may be expressed

$$z - b = - (1/2p) (x - a)^2 \tag{3}$$

where [a, b] are the apogee coordinates and p is a constant known as the semilatus rectum. There are about 100 measured trajectory data points [ $x_i = x(t_i)$ ,  $z_i = z(t_i)$ ]

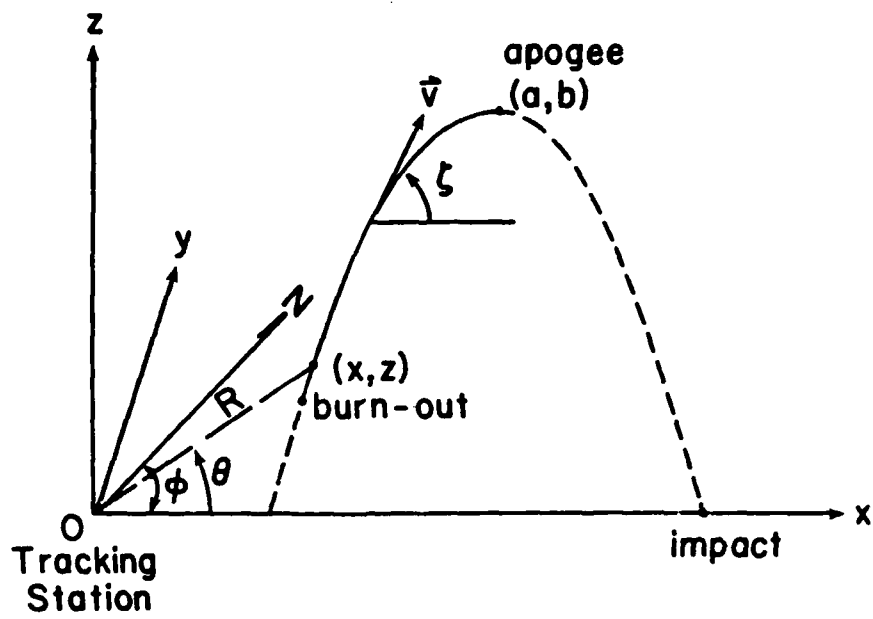


Figure 4. Coordinate System for the Rocket Trajectory

between burn-out and apogee. This data is used to find a "best fit" parabola by calculating

$$A_i = (1/2p) = -(z_i - b')/(x_i - a')^2 \quad (4)$$

where  $[a', b']$  is an estimate of the apogee coordinates, then computing the average

$$\langle A \rangle = (\sum A_i)/N, \quad (5)$$

and finally, forming the mean square difference

$$MSD = [ \sum (A_i - \langle A \rangle)^2 ]/N \quad (6)$$

This process is repeated, using new estimates for  $[a', b']$ , until coordinates  $[a, b]$  are found, which makes the MSD a minimum. Then  $\langle A \rangle$  and  $[a, b]$  are the "best fit" constants for the parabola:

$$z = -\langle A \rangle (x - a)^2 + b. \quad (7)$$

There was no explicit measurement of the rocket orientation, although it is crucial to determining the fraction of the TE and TM fields received on each orthogonal loop. Instead, it was assumed, since the rocket did not leave the atmos-

sphere, that the fins would constrain the rocket axis to coincide with the total velocity vector,  $V$ , tangent to the trajectory. The flight elevation angle can be calculated from Eq. (7):

$$\zeta = \tan^{-1} [-2\langle A \rangle (x - a)] \quad (8)$$

where  $\zeta$  is the angle between the horizontal and the total velocity vector.

Eqs. (7) and (8) express rocket altitude and flight elevation angle as functions of  $x$ , the horizontal distance. However, the trajectory data are obtained as a function of time, that is,  $R = R(t)$ ,  $\theta = \theta(t)$ , and  $\varphi = \varphi(t)$ . The relation between  $x$  and  $t$  for a parabola is simply

$$x(t) = Bt + C \quad (9)$$

The constants  $B$ ,  $C$  can be determined by linear regression using the measured values  $[x_i, t_i]$ . Then

$$z(t) = -\langle A \rangle (Bt + C - a)^2 + b \quad (10)$$

and

$$\zeta(t) = \tan^{-1} [-2\langle A \rangle (Bt + C - a)] \quad (11)$$

Eq. (10) can be used to transform the TE and TM channel output voltages to functions of altitude.

The fraction of a "pure" TE or TM mode actually received on each channel can be determined using Eq. (11) in conjunction with the source azimuth,  $\xi$ , and the azimuth of the rocket trajectory,  $\varphi$ . The TM magnetic field vector from a TM source at azimuth  $\xi$  is

$$H_m = H_{0m} [\sin(\varphi - \xi) \hat{x} + \cos(\varphi - \xi) \hat{y}] \quad (12)$$

where  $H_{0m}$  is the magnitude of the incident field (in ampere/meter). To find the fraction of the total TM field in the direction of the TM antenna axis, denoted as  $A_{mm}$ , we construct a unit vector  $\hat{b}$  perpendicular to the rocket axis:

$$\hat{b} = -\cos \omega_s t \sin \zeta \hat{x} + \sin \omega_s t \hat{y} + \cos \omega_s t \cos \zeta \hat{z}, \quad (13)$$

where  $\omega_s$  is the angular spin rate of the rocket, then take the dot product of

Eqs. (12) and (13):

$$(\vec{H}_m \cdot \hat{b})/H_{0m} = -\cos \omega_s t \sin \zeta \sin(\varphi - \xi) + \sin \omega_s t \cos(\varphi - \xi) \quad (14)$$

The spin modulates the magnitude of this component. The rms value is

$$A_{mm} = [(\vec{H}_m \cdot \hat{b})_{rms}] / H_{0m} = \frac{\sqrt{1 - \sin^2(\varphi - \xi) \cos^2 \zeta}}{\sqrt{2}} \quad (15)$$

A unit vector in the direction of the TE antenna axis (along the rocket axis) is given by

$$\hat{\omega} = \cos \zeta \hat{x} + \sin \zeta \hat{z} \quad (16)$$

so the fraction of TM field in direction  $\hat{\omega}$  is the dot product

$$A_{me} = (\vec{H}_m \cdot \hat{\omega}) / H_{0m} = \sin(\varphi - \xi) \cos \zeta \quad (17)$$

The magnetic field from a TE source has both vertical and longitudinal components, but everywhere except very close to the ground, the vertical component dominates:

$$\vec{H}_e = H_{0e} \hat{z} \quad (18)$$

where  $H_{0e}$  is the magnitude of the incident (vertical) field. The fraction in the TM antenna axis direction is

$$(\vec{H}_e \cdot \hat{b}) / H_{0e} = \cos \omega_s t \cos \zeta \quad (19)$$

which varies due to spin.

The effective (rms) value is

$$A_{em} = [(\vec{H}_e \cdot \hat{b})_{rms}] / H_{0e} = \frac{\cos \zeta}{\sqrt{2}} \quad (20)$$

In the TE antenna axis direction, the fraction is

$$A_{ee} = (\vec{H}_e \cdot \hat{\omega}) / H_{0e} = \sin \zeta \quad (21)$$

#### 4. DATA REDUCTION

At the conclusion of the launch campaign, there existed an analog data tape containing broadband LF/VLF signal voltages from the TM and TE receivers as functions of time. The first step in data reduction was to prepare digital tapes for each frequency of interest. Under the control of a Tektronix 4054 computer, a Nicolet Model 446B Spectrum Analyzer performed FFTs on the broadband analog voltages; by first setting the analyzer bandwidth to 50 kHz, numerous signals usually could be observed on the 400-point display, in most cases corresponding to known ground-based or airborne sources. Next, using higher resolution, a 2 kHz bandwidth was displayed, centered on a frequency of interest. We selected 20 points (bandwidth = 100 Hz) for the noise and 5 points (25 Hz) for the signal, averaged each set of points, and recorded the averages once per second for the duration of the 4-min flight. A flow chart of the data reduction steps is shown in Figure 5.

The next step was to plot and compare the signal and noise averages to deter-

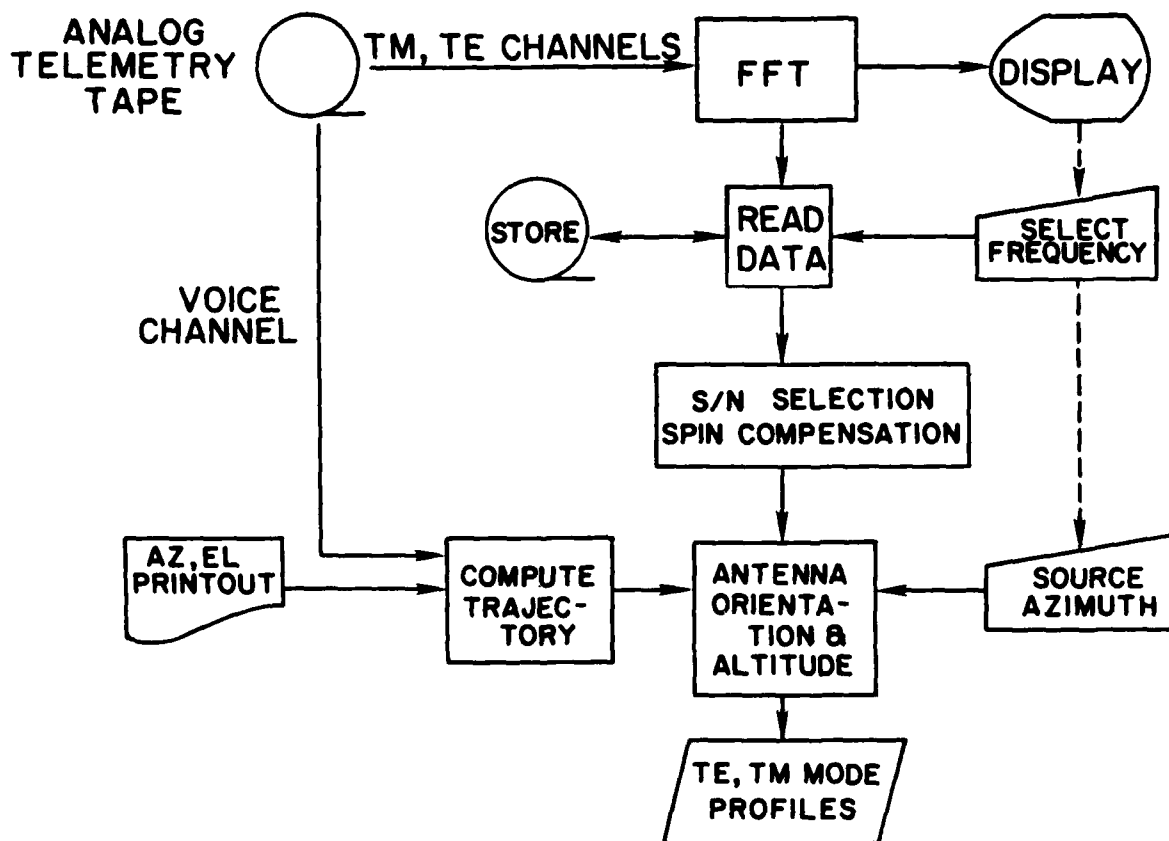


Figure 5. Data Reduction Flow Chart for Mode Profile Analysis

mine whether an adequate signal-to-noise ratio (S/N) existed for the measurements. We assumed that if  $S/N > 6$  dB, we could process the signal data without having to correct for noise contamination.

The signals in each channel actually were due to a combination of TE and TM fields because of rocket orientation and spin. Since the rocket was only slightly tilted from vertical for most of the upward portion of the flight, we assumed as a first approximation that each channel's signal was unaffected by the orthogonal polarization. Initial estimates of TE and TM field strengths then were made simply by applying  $A_{mm}$  and  $A_{ee}$  to adjust for the small tilt. To test the validity of these estimates, we calculated the cross-coupling expected in each channel, using the initial estimates and applying the appropriate cross-geometric factors  $A_{me}$  and  $A_{em}$ . We assumed that the first approximation was indeed a good estimate of the field so long as the calculated cross-coupling was 6 or more dB smaller than the actual recorded channel voltage. Where this was not the case, the first approximation was considered to be invalid, and we made no claim for a measurement of that component.

## 5. SIGNAL SOURCES, LOCATIONS, AND PROPAGATION PATHS

Within the 15 to 50 kHz bandwidth of the rocket receivers, 14 VLF/LF signals were detected ( $S/N > 6$  dB) on at least one channel over some portion of the flight. Thirteen of these, found between 15 and 27 kHz, can be seen in Figure 6; this composite spectrum was obtained by repeatedly playing the analog tape and selecting 2 kHz spectra viewed on the analyzer when the signals appeared to be the strongest. Due to the spin of the TM antenna, the spectra of sufficiently narrow signals (bandwidth  $<$  spin frequency) are observed to be split into two lines, each with half the

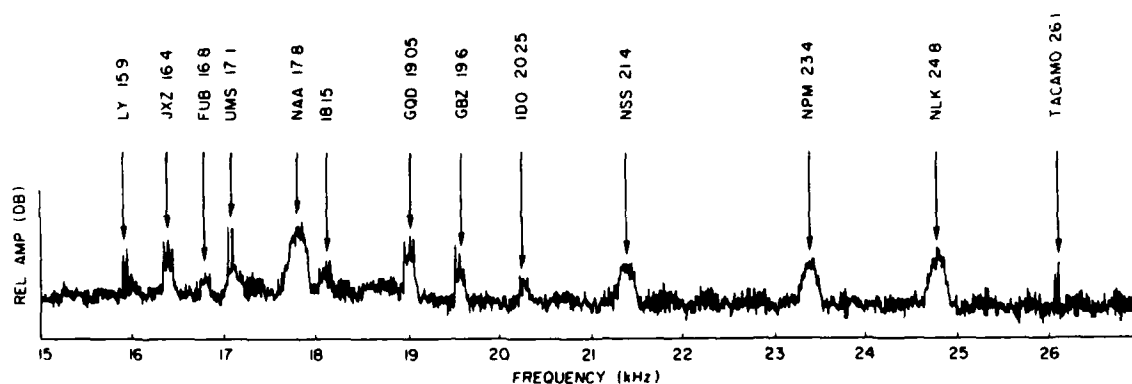


Figure 6. Composite Spectrum of Received TM Signals

energy of the original line. On the other hand, signals whose bandwidths are much wider than the spin frequency, that is, "spread spectrum" signals, show only a small increase in width since only lines at or near the edges are displaced outside the original spectrum. Of the 14 detected signals, 13 tentatively were identified by frequency as specific LF/VLF transmitters; their propagation paths to Thule are shown in Figure 7, and certain relevant parameters are given in Table 1.

All the identified sources except TACAMO used ground-based vertical antennas. The TACAMO aircraft was flying at 20,000 ft over the western Atlantic, on a heading approximately perpendicular to the azimuth of Thule and at sufficiently high speed to cause its trailing-wire antenna to assume a nearly horizontal orientation broadside to the TACAMO-to-Thule propagation path.

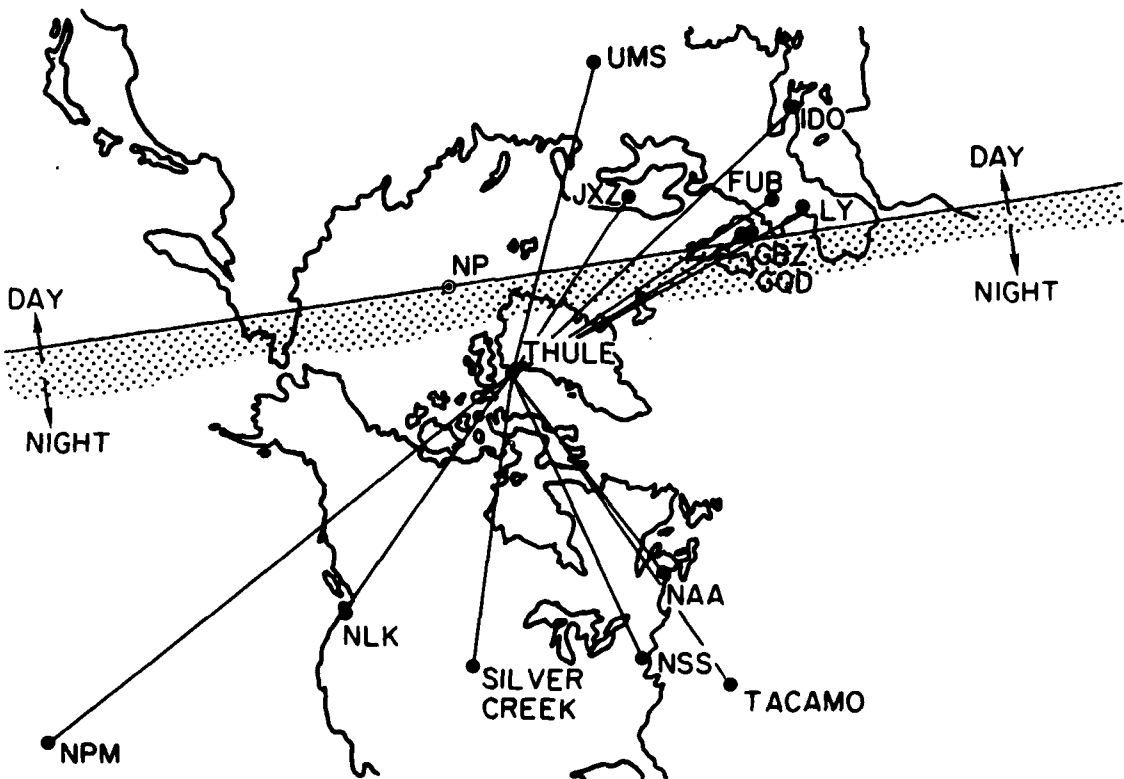


Figure 7. Propagation Paths to Thule. On 21 September, the day/night terminator passed through the North Pole (NP)

Table 1. Transmitter Listing by Frequency

Measured Frequency (kHz)	Source Call	Identification Location	Azimuth at Thule	Propagation Distance (kM)	ERP (kW)
15.9	LY	Bordeaux, France	098	4640	33
16.4	JXZ	Aldra, Norway	068	2810	[NA]
16.8	FUB	St. Assisse, France	093	4260	30
17.1	UMS	Gorki, U.S.S.R.	048	4530	315
17.8	NAA	Cutler, Maine	178	3550	1000
18.15		[Unknown]			
19.05	GQD	U.K.	096	3740	[NA]
19.6	GBZ	Criggion, U.K.	096	3740	10
20.25	IDO	Rome, Italy	086	5260	[NA]
21.4	NSS	Annapolis, Md.	190	4180	266
23.4	NPM	Haiku, Hawaii	275	7670	530
24.8	NLK	Jim Creek, Wash.	248	3900	234
26.1	TACAMO	38°N, 72°W	184	4280	100
48.5	[NA]	Silver Creek, Nebr.	217	4140	50

## 6. HEIGHT PROFILES

In Figures 8 to 16, height-gain profiles of 9 of the 14 detected sources are shown. In each of the figures:

(1) The abscissa is given in dB relative to 1  $\mu$ V/m, indicating that voltage-to-field strength calibrations have been applied (the spin of the TM antenna has been taken into account by multiplying the TM signal strength by  $\sqrt{2}$ ).

(2) In (a) and (c), the solid curves are the raw signal strength plus noise, while the dashed curves are noise alone at a slightly detuned frequency.

(3) In (b) and (d), the final estimates of the TM and TE field strengths are obtained using Eqs. (15) and (21).

(4) Profiles are drawn only where both the signal-to-noise and the recorded signal-to-calculated cross-coupling ratios equal or exceed 6 dB.

In part (b) of Figures 10, 15, and 16, the arrow marks the signal strength measured on the ground at launch.

A significant feature seen in all the profiles is the high background noise over the first 20 km of altitude, apparently due to the burning solid fuel ARCAS rocket motor. This noise tends to mask signals in that altitude range. (The S/N ratio of the strongest signal recorded, NAA at 17.8 kHz, did exceed +6 dB on the TM chan-

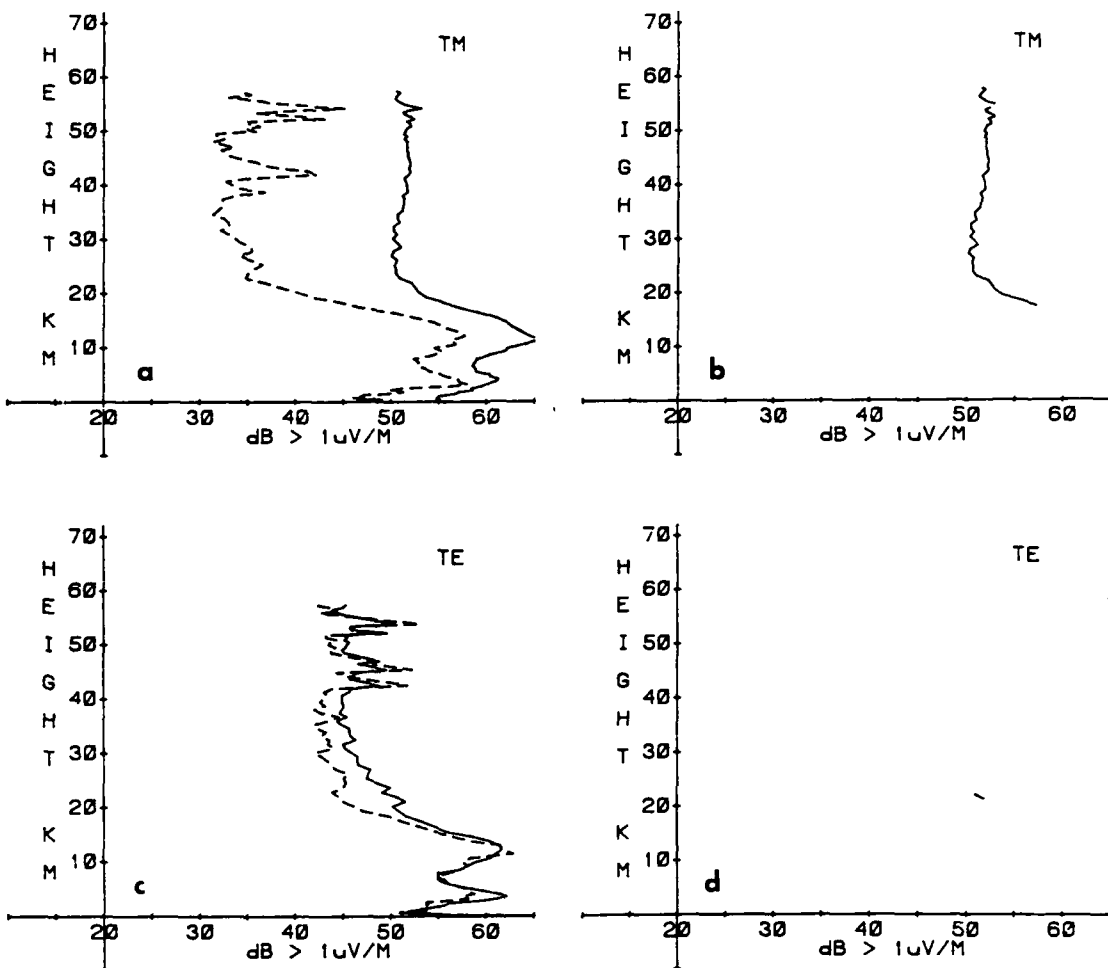


Figure 8. Height-Gain Profiles for 16.4 kHz (JXZ): (a) Recorded TM Signal (Solid Line) and Noise (Dashed Line); (b) TM Signal Compensated for Rocket Tilt; (c) Recorded TE Signal (Solid Line) and Noise (Dashed Line); (d) TE Signal Compensated for Rocket Tilt

nel, but the curves for the other transmitters have large gaps where the S/N ratio was too small.) Above 20 km, where the rocket motor was no longer firing, the noise is 20 dB or so smaller on both channels, and many signals that had been obscured now stand out clearly.

## 7. DATA ANALYSIS AND DISCUSSION

For each of the nine transmitters, Table 2 gives solar illumination, ground path, and whether TM and/or TE signals were recorded during the rocket flight. The first eight sources listed are the ground-based TM transmitters. TM signals

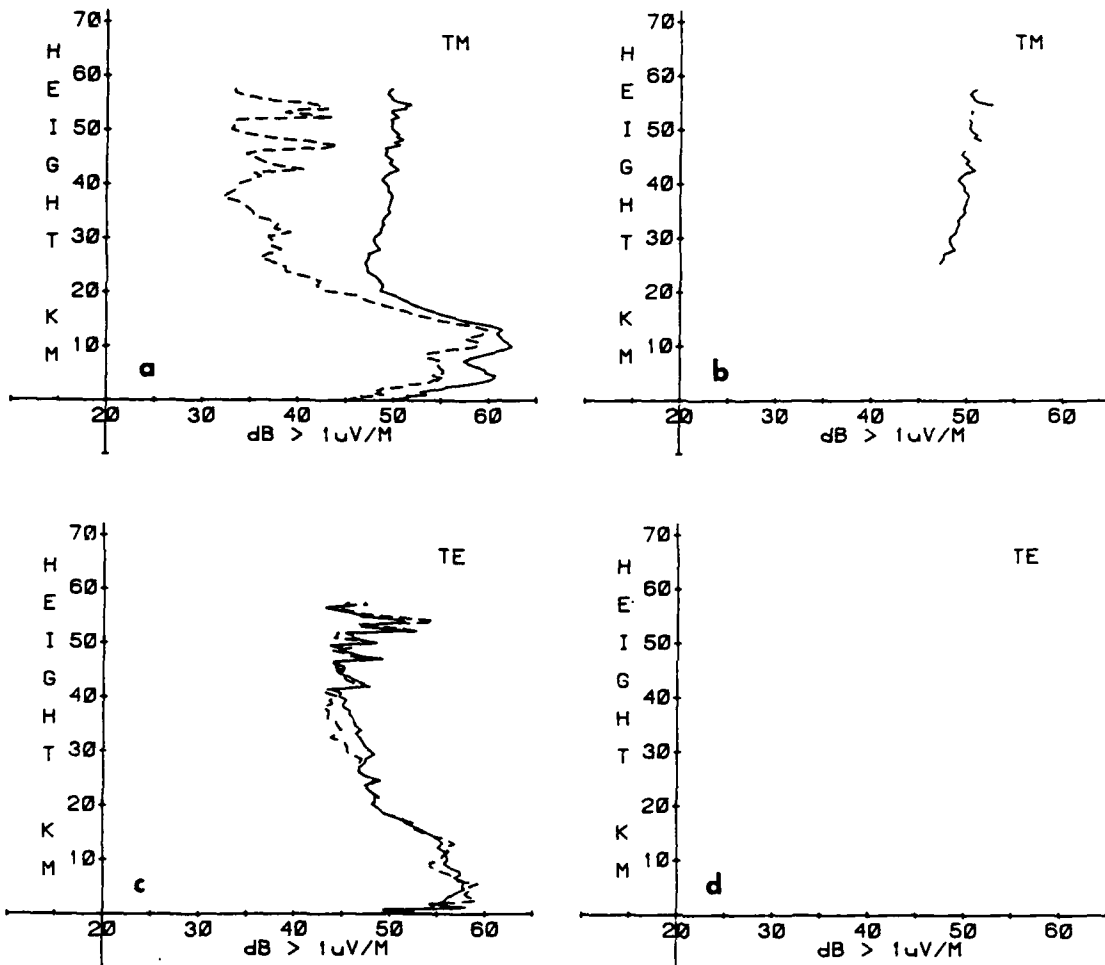


Figure 9. Height-Gain Profiles for 17.1 kHz (UMS): (a) Recorded TM Signal (Solid Line) and Noise (Dashed Line); (b) TM Signal Compensated for Rocket Tilt; (c) Recorded TE Signal (Solid Line) and Noise (Dashed Line); (d) TE Signal Compensated for Rocket Tilt

were received from each of these, irrespective of propagation conditions. On the other hand, converted signals (TE) were seen from only four of these sources, specifically those with propagation paths that were entirely under nighttime conditions and that did not cross over the Greenland ice cap. For those transmitters, the TE fields usually were somewhat weaker than the corresponding TM fields, although at aircraft altitudes, they were of the same order of magnitude. The other four sources, for which no converted signals were measured, had propagation paths involving the day/night terminator and that crossed the ice cap as well.

The presence of TE signals from ground-based transmitters (which do not radiate TE polarization) is due to conversion by the geomagnetic field. The amount of this conversion depends in part on the effective height of the upper (ionospheric)

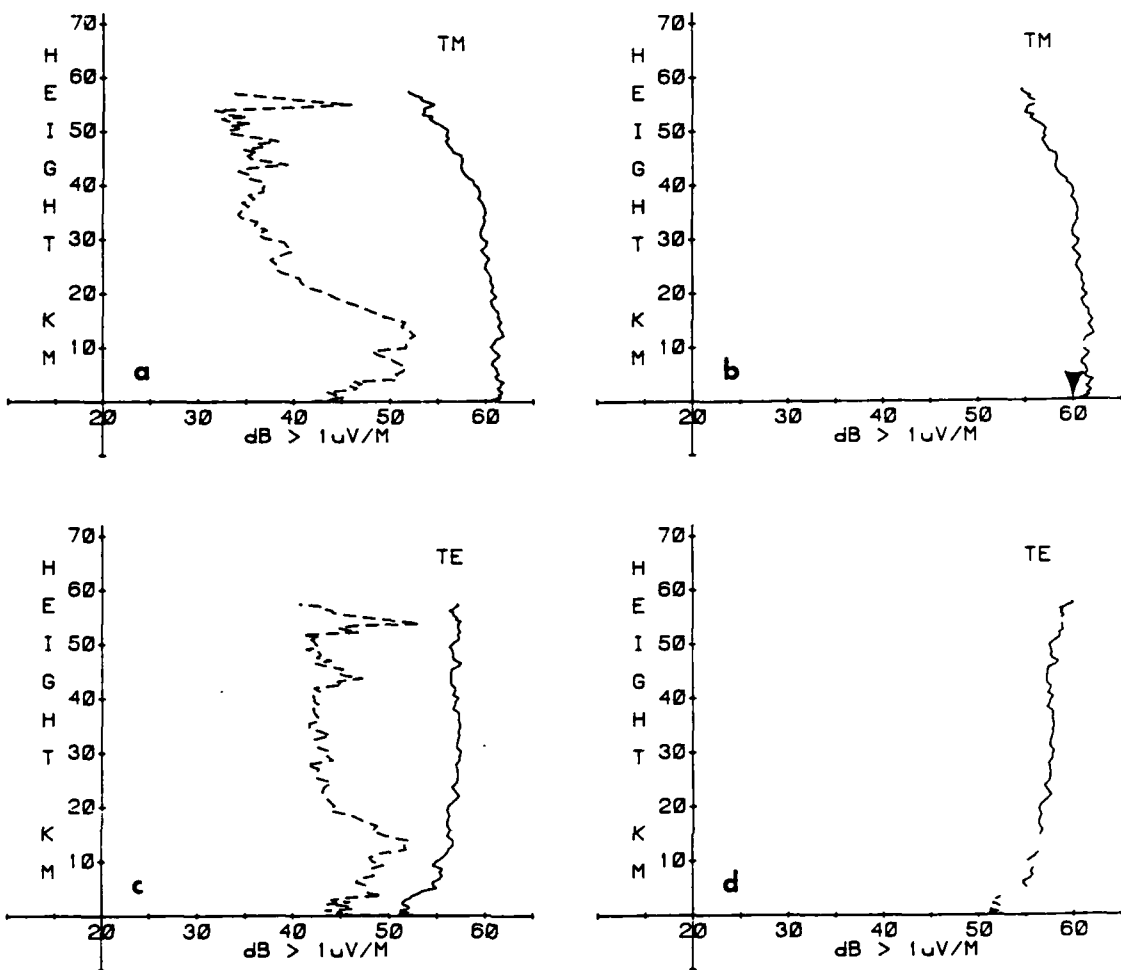


Figure 10. Height-Gain Profiles for 17.8 kHz (NAA): (a) Recorded TM Signal (Solid Line) and Noise (Dashed Line); (b) TM Signal Compensated for Rocket Tilt; (c) Recorded TE Signal (Solid Line) and Noise (Dashed Line); (d) TE Signal Compensated for Rocket Tilt

boundary. At nighttime the upper boundary is high, and there is more conversion of TM to TE than during the daytime when the ionosphere is lower. Because theoretical considerations imply conversion all along the propagation path, the absence of a measured TE signal from transmitters in the daytime hemisphere may indicate the possible influence of mode excitation at the day/night boundary and/or reduced coupling between TE and TM modes over the Greenland ice cap. This would be a good area for additional theoretical and experimental investigations.

The last source listed in Table 2 is the airborne TACAMO transmitter, which radiated both TM and TE due to the inclination of the trailing-wire antenna. The height-gain profiles (Figure 16a, 16c) show that the observed TE fields were much stronger than the TM fields (48 vs 39 dB > 1  $\mu$ V/m). The TM signal, which was

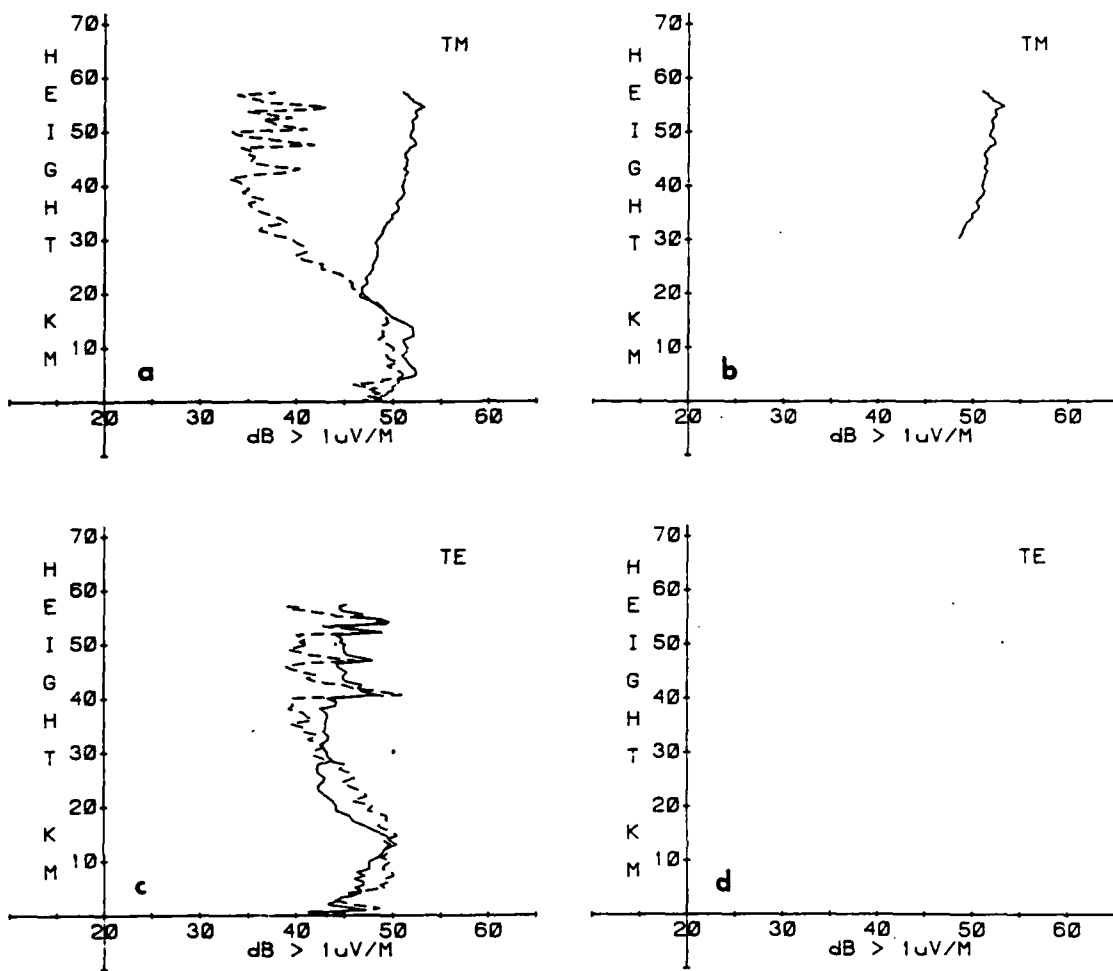


Figure 11. Height-Gain Profiles for 19.05 kHz (GQD): (a) Recorded TM Signal (Solid Line) and Noise (Dashed Line); (b) TM Signal Compensated for Rocket Tilt; (c) Recorded TE Signal (Solid Line) and Noise (Dashed Line); (d) TE Signal Compensated for Rocket Tilt

larger than the 36 dB  $> 1 \mu\text{V/m}$  signal observed by the ground receiver, most likely was cross-coupled TE due to rocket tilt; thus, no TM profile is shown in Figure 16b. This absence of measured TM indicates very little magneto-ionic conversion of TE to TM, in contrast to the significant TM to TE conversion observed for ground-based transmitters with similar propagation paths (that is, nighttime, no ice cap).

It is important to note that the TE signal strengths (converted TM) from the ground-based transmitters in the nighttime hemisphere were equal to or were larger than the TE signals received from TACAMO. Although consideration must be given to account for effects due to differences in radiated power, frequency, range, or path parameters for the sources, this observation has strong implica-

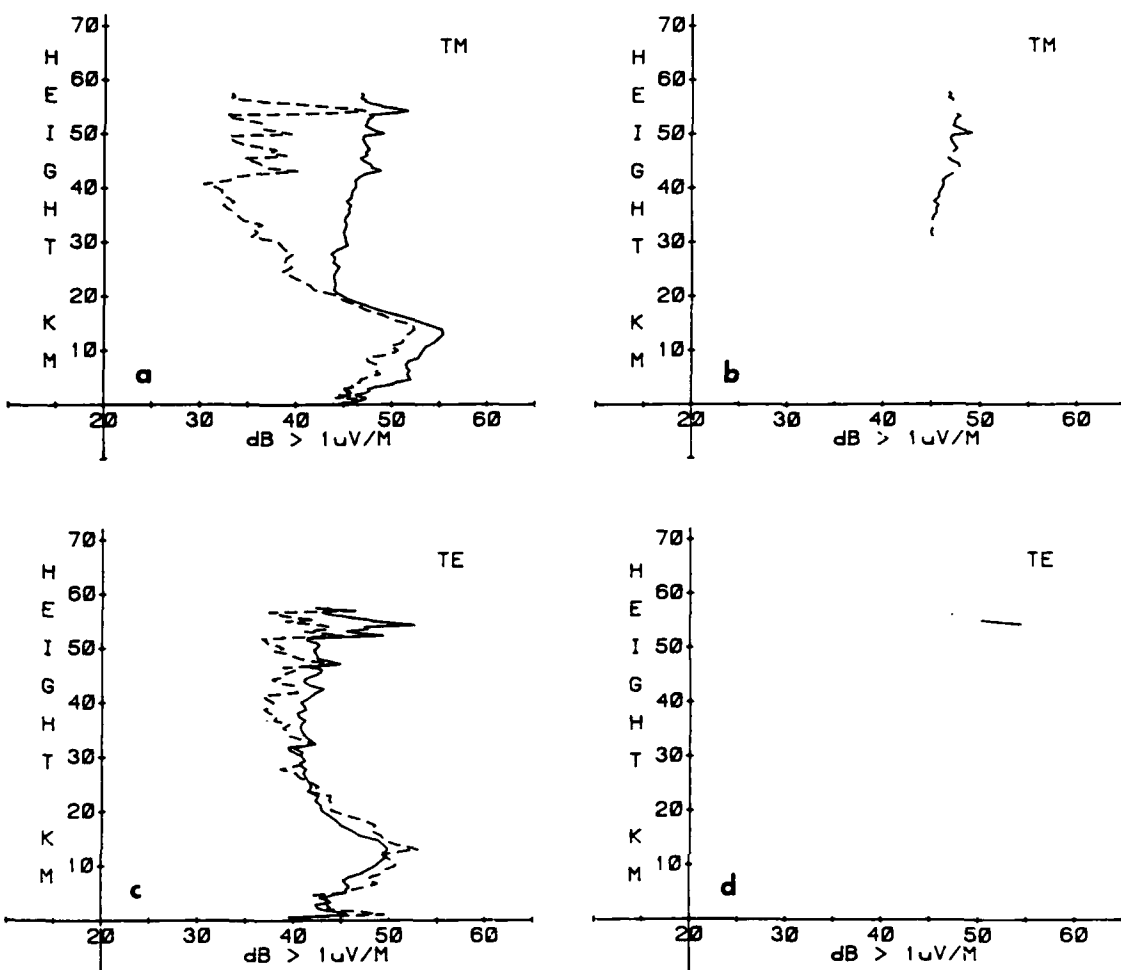


Figure 12. Height-Gain Profiles for 19.6 kHz (GBZ): (a) Recorded TM Signal (Solid Line) and Noise (Dashed Line); (b) TM Signal Compensated for Rocket Tilt; (c) Recorded TE Signal (Solid Line) and Noise (Dashed Line); (d) TE Signal Compensated for Rocket Tilt

tions in the assessment of coverage of airborne systems in the presence of other signals.

A feature noticed in the TM height profiles is the tendency for those which cross the ice cap (Figures 8, 9, 11, 12) to become stronger with altitude, while those not crossing the cap (Figures 10, 13, 14, 15) become weaker with altitude. The signals from the two transmitters in the United Kingdom (Figures 11, 12) show this trend quite clearly, the amplitudes increasing by more than 10 dB as the altitude increases from 20 km to 60 km. Waveguide calculations<sup>6</sup> show that TM profiles

---

6. Field, E.C., Jr., and Warber, C.R., Pacific-Sierra Research Corp., Los Angeles, Calif. (1985) Private communication.

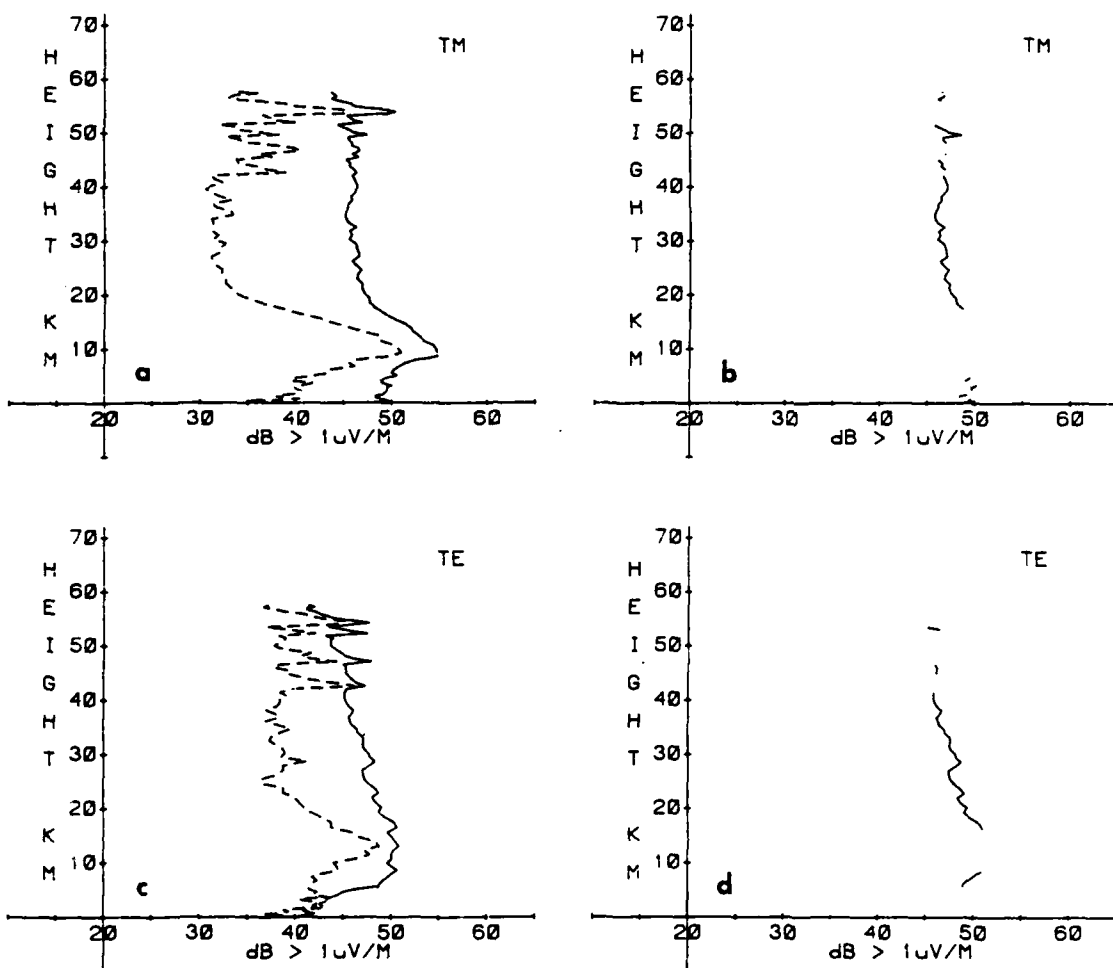


Figure 13. Height-Gain Profiles for 21.4 kHz (NSS): (a) Recorded TM Signal (Solid Line) and Noise (Dashed Line); (b) TM Signal Compensated for Rocket Tilt; (c) Recorded TE Signal (Solid Line) and Noise (Dashed Line); (d) TE Signal Compensated for Rocket Tilt

over "Greenland ice" do indeed increase with altitude (see Figure 17). It appears that the dielectric-like ice cap, in effect, distorts the waveguide fields, displacing the TM maximum from the lower boundary.

The rocket was launched essentially at the boundary between a very good conductor (sea water) and a very poor one (the polar ice cap). The transition region is very abrupt, the conductivity changing many orders of magnitude within a few kilometers (much less than one wavelength at 20 kHz) of the launch site. The data show that the height profiles tend to retain characteristics corresponding to the ground parameters of the entire propagation path, rather than immediately transforming to new profiles as they cross a boundary. Thus, at Thule or other locations where the conductivity changes abruptly, source azimuth is more important

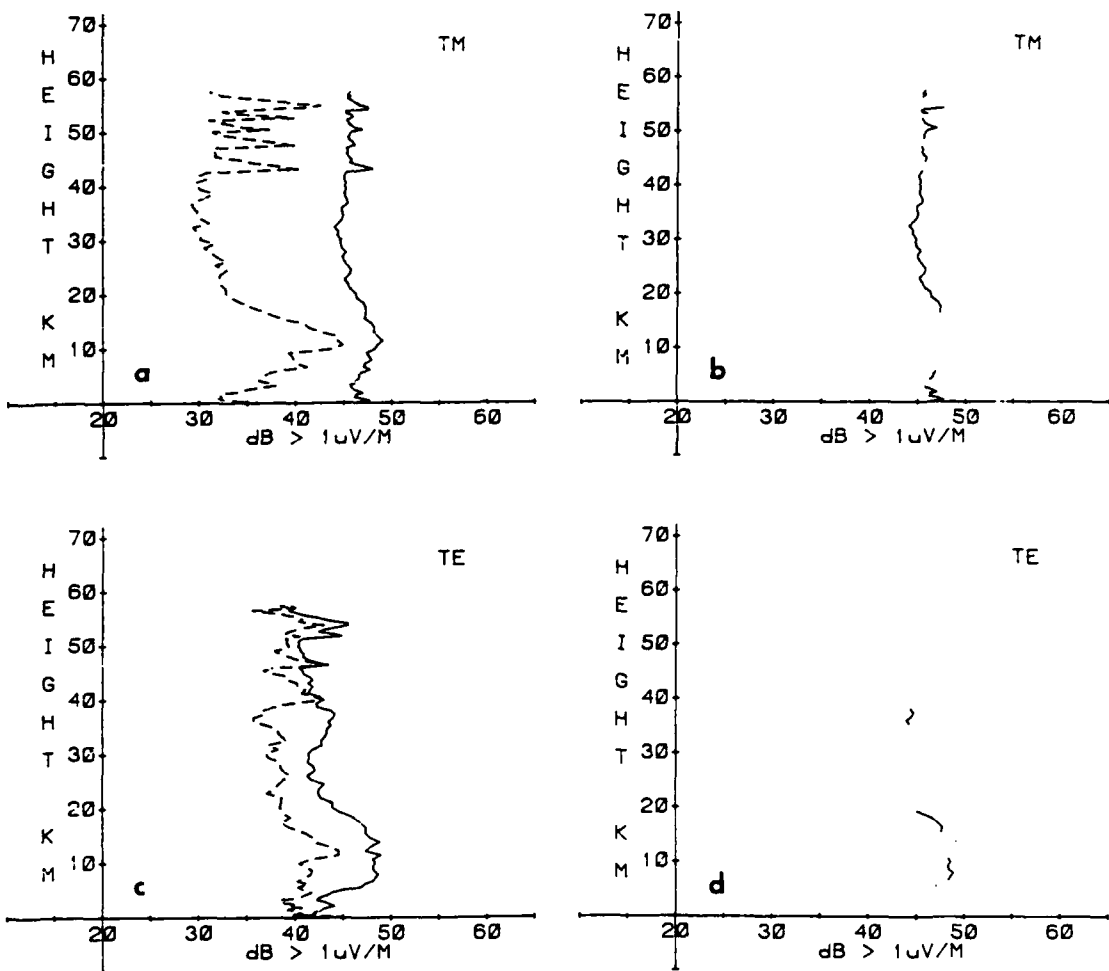


Figure 14. Height-Gain Profiles for 23.4 kHz (NPM): (a) Recorded TM Signal (Solid Line) and Noise (Dashed Line); (b) TM Signal Compensated for Rocket Tilt; (c) Recorded TE Signal (Solid Line) and Noise (Dashed Line); (d) TE Signal Compensated for Rocket Tilt

in determining signal height-gain than is the ground conductivity directly under the receiver.

## 8. CONCLUSIONS

This rocket experiment has provided measured height-gain profiles of nine very low frequency (VLF) signals, at high latitude and under quiet ionospheric conditions. The profiles were shown to depend on ground conductivity and solar illumination conditions on the propagation paths. Conversion of TM to TE was quite evident for paths under total nighttime conditions, while no conversion was ob-

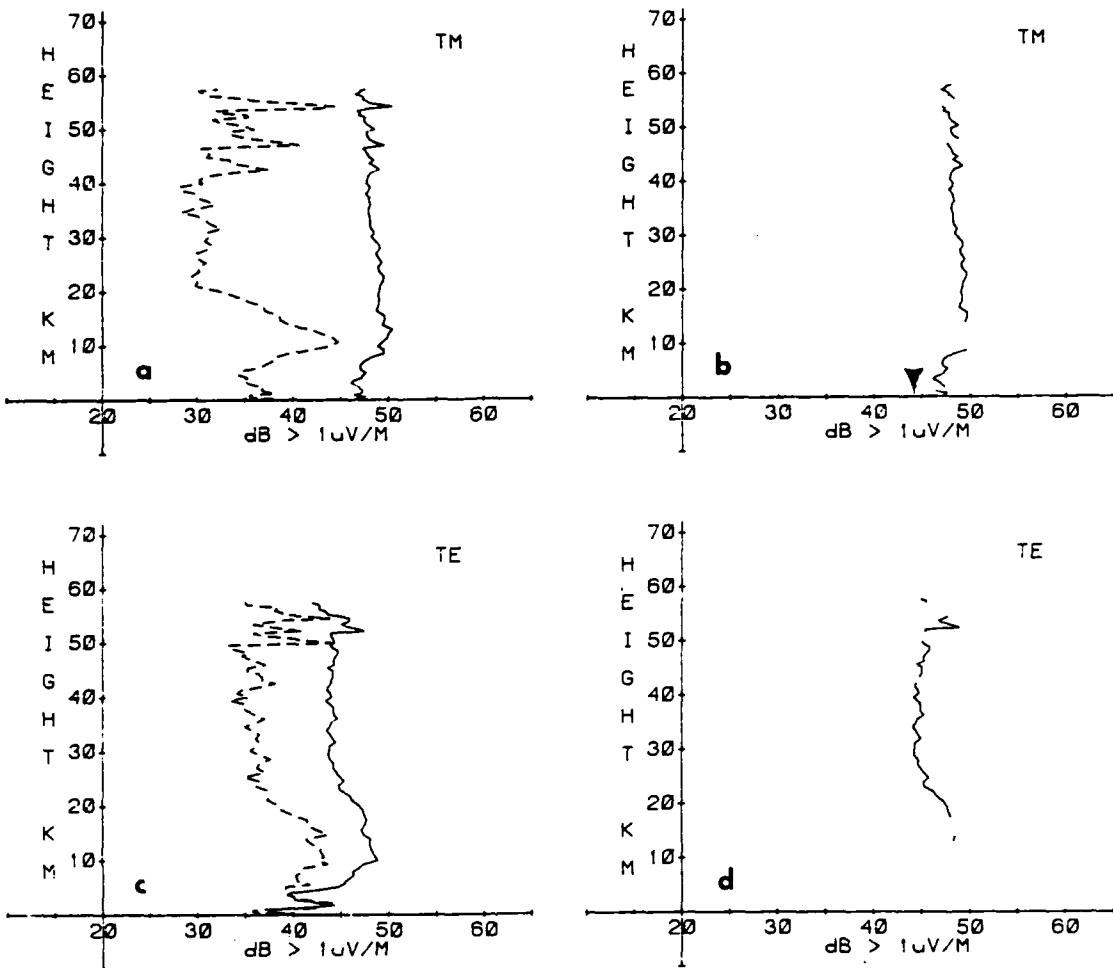


Figure 15. Height-Gain Profiles for 24.8 kHz (NLK): (a) Recorded TM Signal (Solid Line) and Noise (Dashed Line); (b) TM Signal Compensated for Rocket Tilt; (c) Recorded TE Signal (Solid Line) and Noise (Dashed Line); (d) TE Signal Compensated for Rocket Tilt

served on paths for which the transmitter was in daylight. The observation that converted signals from ground-based transmitters were comparable in field strength to TE from an airborne source has important ramifications for assessing communications in the presence of interference. Because of the diverse conditions along the propagation paths for the numerous signals observed during the experiment, another potential and important use of the data is to provide a means by which VLF/LF propagation prediction codes can be validated.

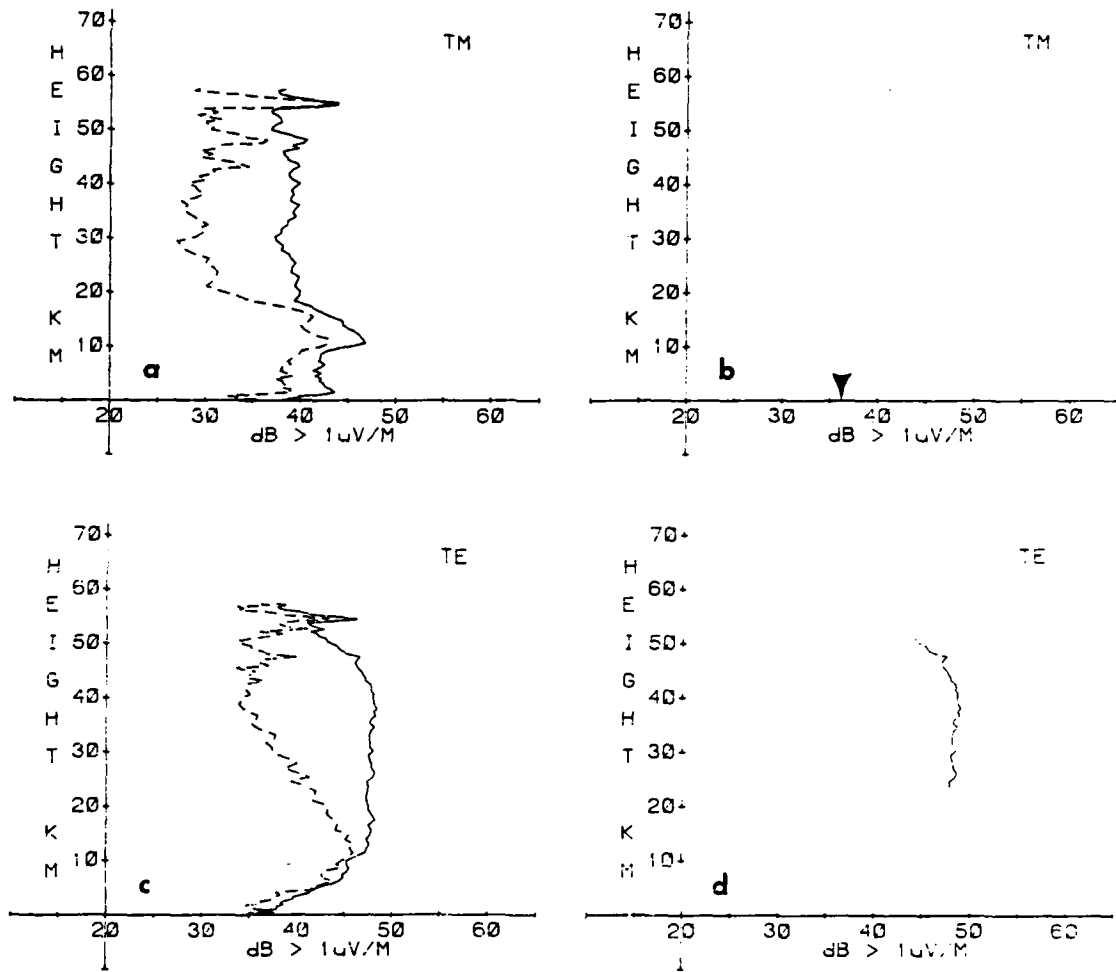


Figure 16. Height-Gain Profiles for 26.1 kHz (TACAMO): (a) Recorded TM Signal (Solid Line) and Noise (Dashed Line); (b) TM Signal Compensated for Rocket Tilt; (c) Recorded TE Signal (Solid Line) and Noise (Dashed Line); (d) TE Signal Compensated for Rocket Tilt

Table 2. Propagation Conditions

Frequency	Source	Path Illumination	Path Over Ice Cap	Received TM	Received TE
16.4	Aldra, Norway	day/night	yes	yes	no
17.1	Gorki, U. S. S. R.	day/night	yes	yes	no
17.8	Cutler, Maine	night	no	yes	yes
19.05	U.K.	day/night	yes	yes	no
19.6	Criiggion, U.K.	day/night	yes	yes	no
21.4	Annapolis, Md.	night	no	yes	yes
23.4	Haiku, Hawaii	night	no	yes	yes
24.8	Jim Creek, Wash.	night	no	yes	yes
26.1	TACAMO	night	no	no	yes

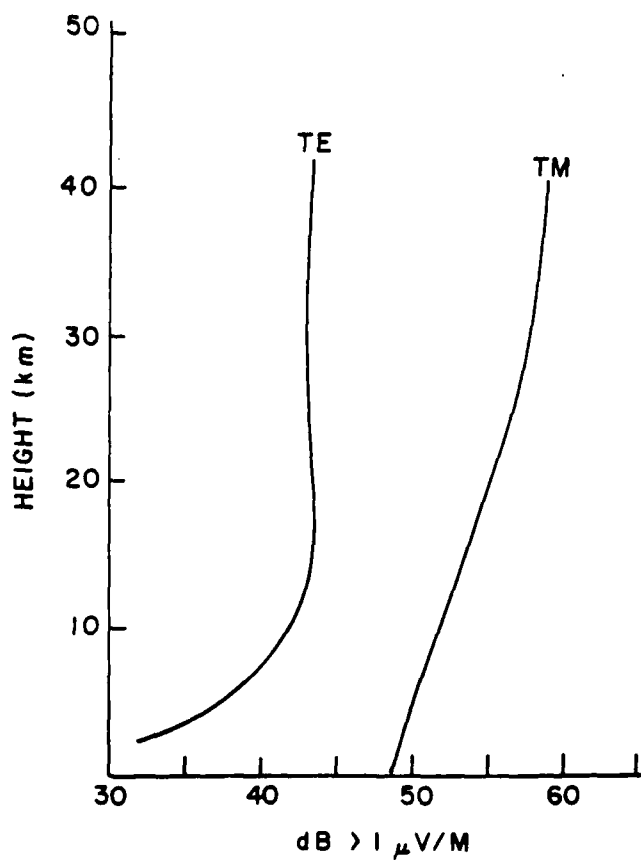


Figure 17. Calculated Height-Gain Profiles for GBZ to Thule

## References

1. Lewis, E.A., and Harrison, R.P. (1975) Experimental Evidence of a Strong, TE-Polarized Wave From an Airborne LF Transmitter, AFCRL-TR-75-0555, AD A019689.
2. Hirst, G.C. (1975) (U) U-2 investigations of a new mode for LF air-to-air communications, in Proc. AFSC 1975 Science and Engineering Symposium, AFSC-TR-75-06 (Vol. 1), AD A021660.
3. Harrison, R.P., Lewis, E.A., Donohoe, J.B., and Rasmussen, J.E. (1981) TM/TE Polarization Ratios in a Sample of 30kHz Sferics Received at Altitudes From 0 to 70km, RADC-TR-81-235, AD A108182.
4. Field, E.C., Jr., Warber, C.R., Kossey, P.A., Lewis, E.A., and Harrison, R.P. (1986) Comparison of calculated and measured height profiles of transverse electric VLF signals across the daytime Earth-ionosphere waveguide, Radio Sci. 21(No. 1):141-149.
5. Kossey, P.A., Lewis, E.A., and Field, E.C. (1982) Relative characteristics of TE/TM waves excited by airborne VLF/LF transmitters, in Medium, Long and Very Long Wave Propagation (at frequencies less than 3000kHz), AGARD-CP-305, Dr. J.S. Belrose, Advisory Group for Aerospace Research and Development, North Atlantic Treaty Organization, Ed., AD A113969.
6. Field, E.C., Jr., and Warber, C.R., Pacific-Sierra Research Corp., Los Angeles, Calif. (1985) Private communication.

END

DATE

FILED

8-88

DTIC